Basic of SEERS Implementation
at
Hercules measurement systems

Michael Klick
ASI Advanced Semiconductor Instruments GmbH
Rudower Chaussee 30
12489 Berlin

ADVANCED SEMICONDUCTOR INSTRUMENTS

Contents

Plasma Monitoring with SEERS

parameter

- electron density
- electron collision rate
- plasma bulk power

rf sensor

- passive
- non intrusive
- easy to install
- reversible
- tolerant to deposited layers

information

- absolute values
- volume averaged values
- SECS/Brookside/Customer communication moduls

Limitation and possibilities of process monitoring

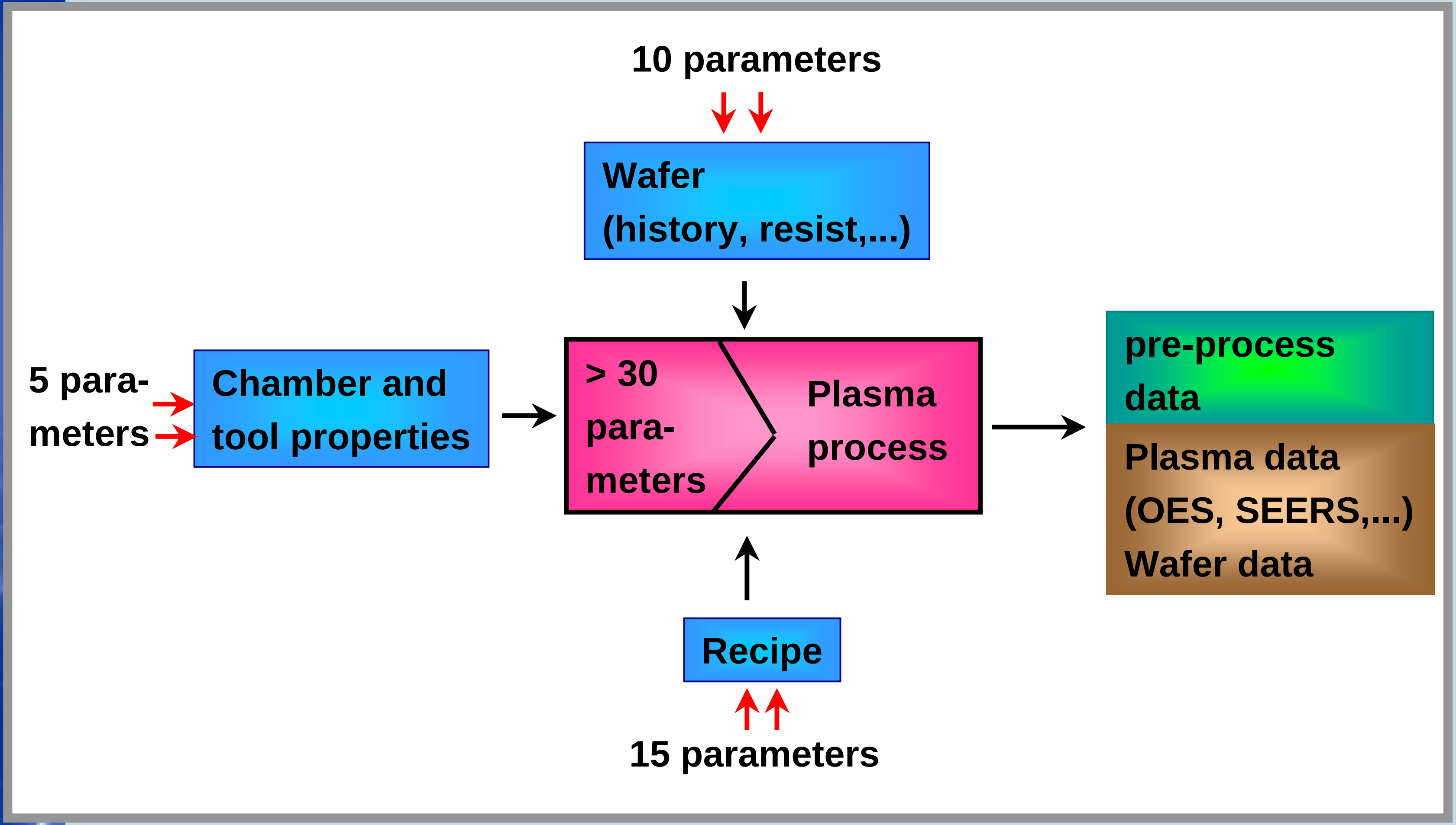

Principle and experimental setup

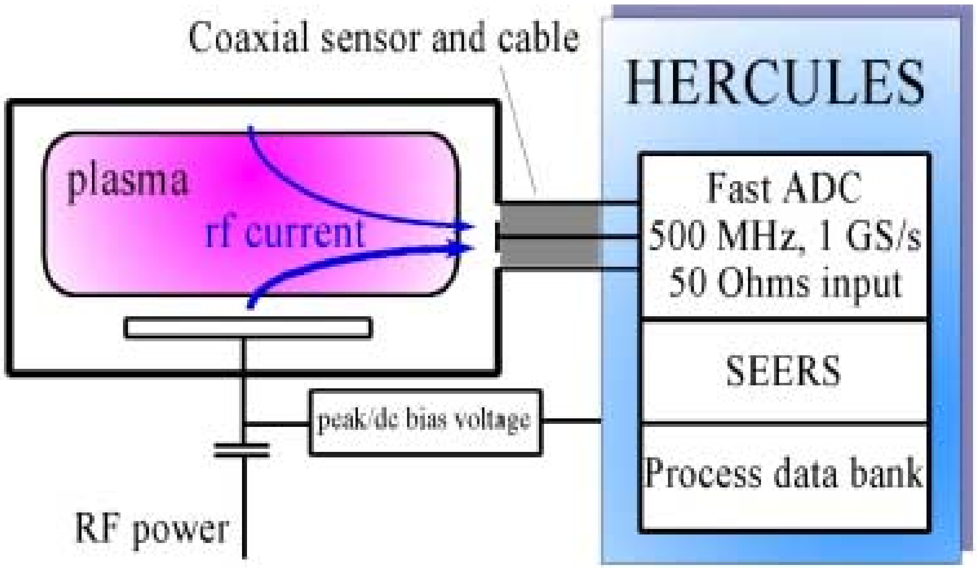

rf current
rf voltage

↓

FFT

↓

Model SEERS

↓

Electron collision rate
Electron density
Bulk power
DC bias voltage

- ***Passive*** electrical method, no influence on the plasma
- ***Integral*** measurement

SEERS - an easy explanation

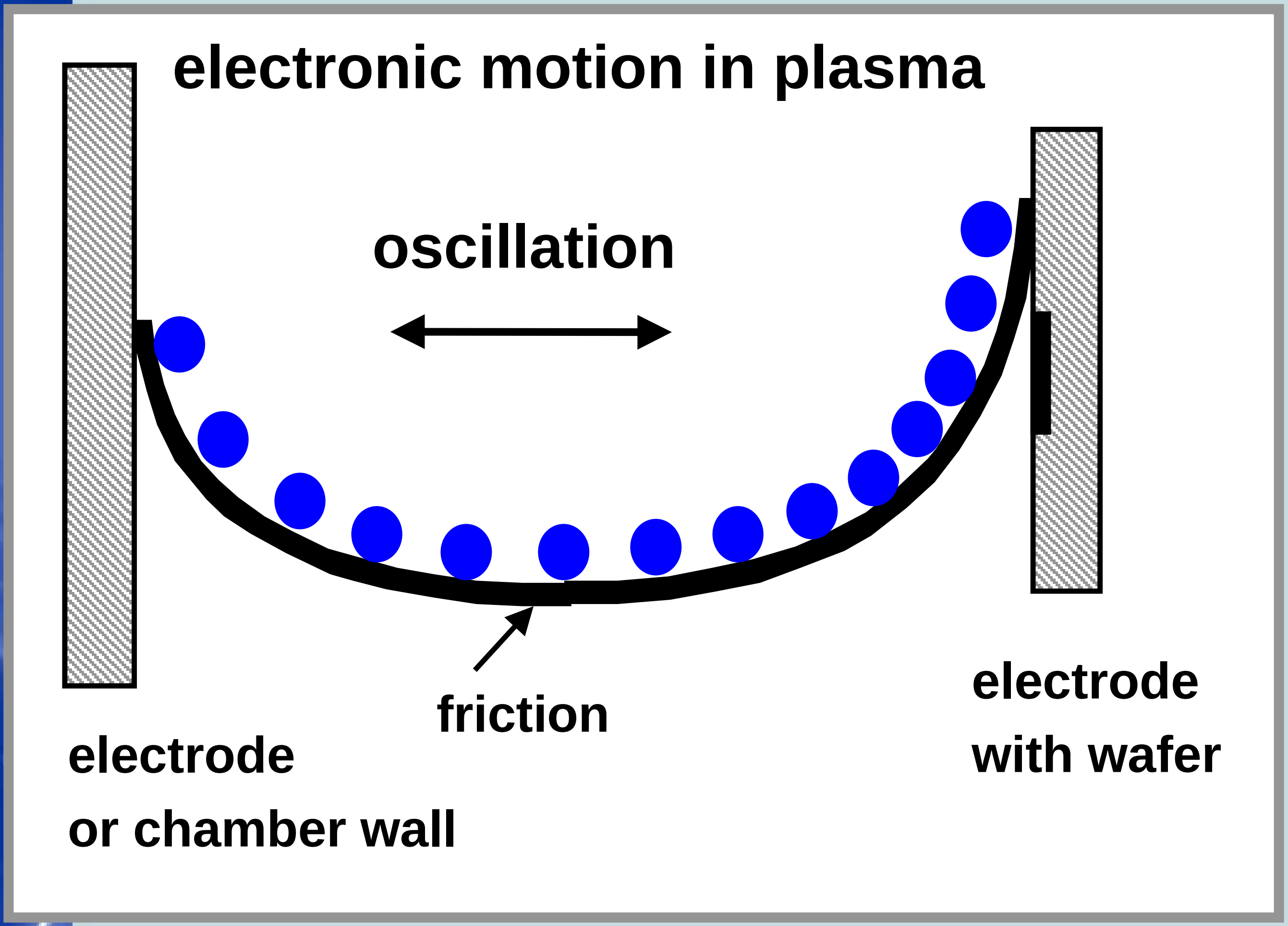

Hercules: A SEERS Implementation

Mechanical analogon of SEERS

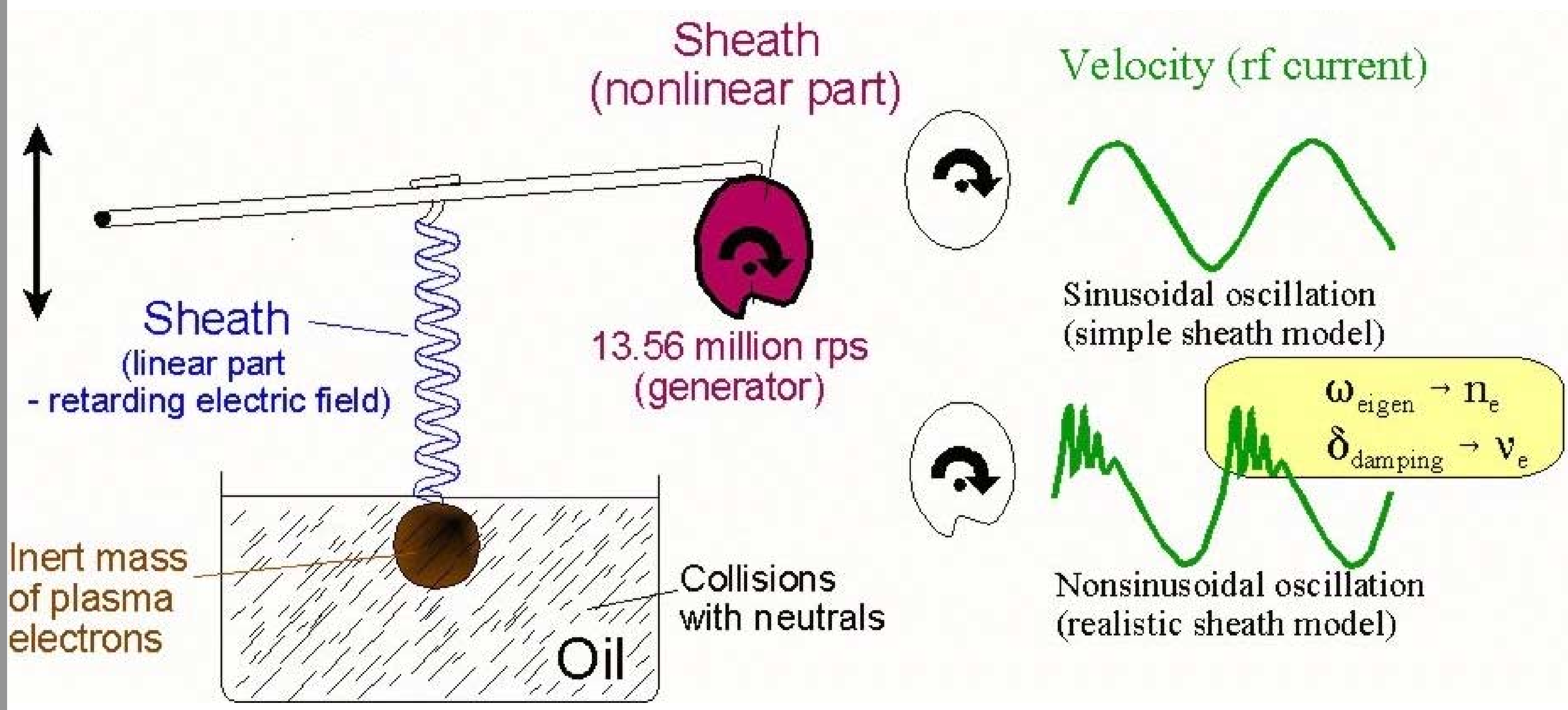

Self Excited Electron Resonance Spectroscopy

Discharge current

Measured and calculated current in Ar

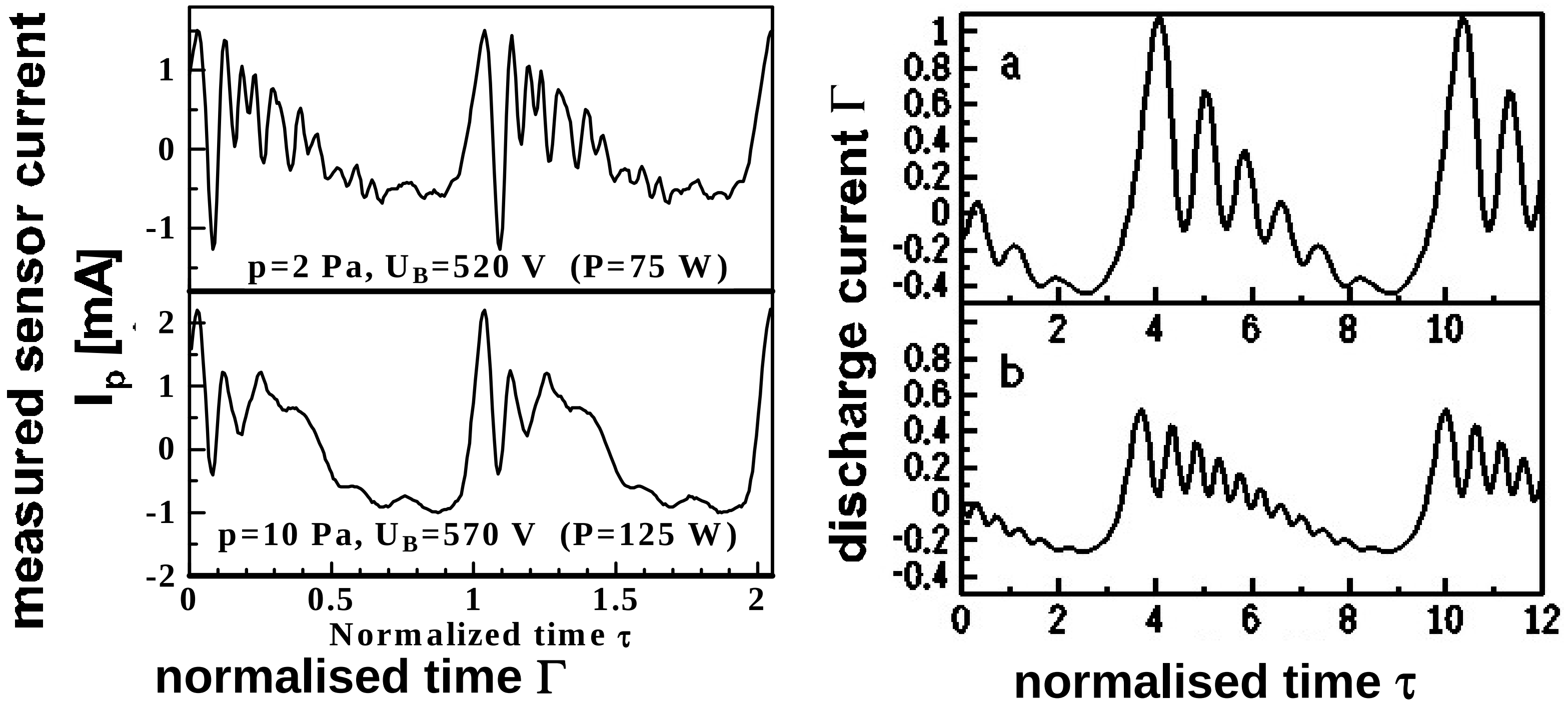

a) Ω = 0.05, ρ = 8, Δ = 6,

b) Ω = 0.03, ρ = 4, Δ = 3,

$\hat{\eta} = U/U_{Te} = 100$, $\hat{\eta}_B = U_B/U_{Te} = 100$

Source: M. Klick et al., Jpn. J. Appl. Phys., Part I, 36(1997)7B, 4625.

Basic HERCULES Model

High Frequency Electron Resonance Current Low Pressure Spectroscopy

Matchbox and generator

HERCULES equivalent circuit

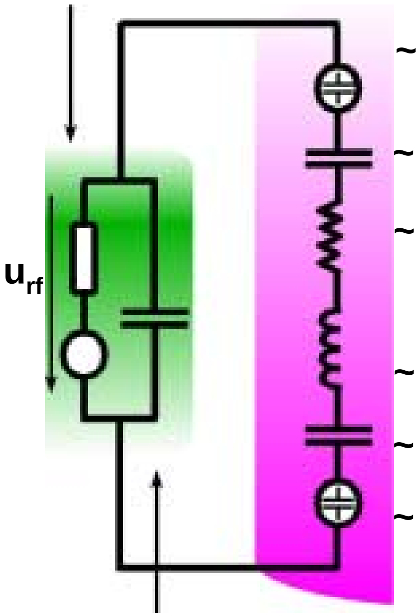

~ u_1 [-∫i dt]	nonlinearity sheath plasma-wall
~ S_1	linear „part“ of wall sheath
~ $\nu l m_e$	ohmic part of plasma bulk (ohmic and stoachastic heating)
~ $\omega\ l\ m_e$	inertia (imaginary) part thereof
~ s_0	linear „part“ of rf sheath
~ u_0 [∫i dt]	nonlinearity sheath rf electrode

Feed-through and stray capacitance

Basic equations

RF current distribution of cylindrical RF discharge

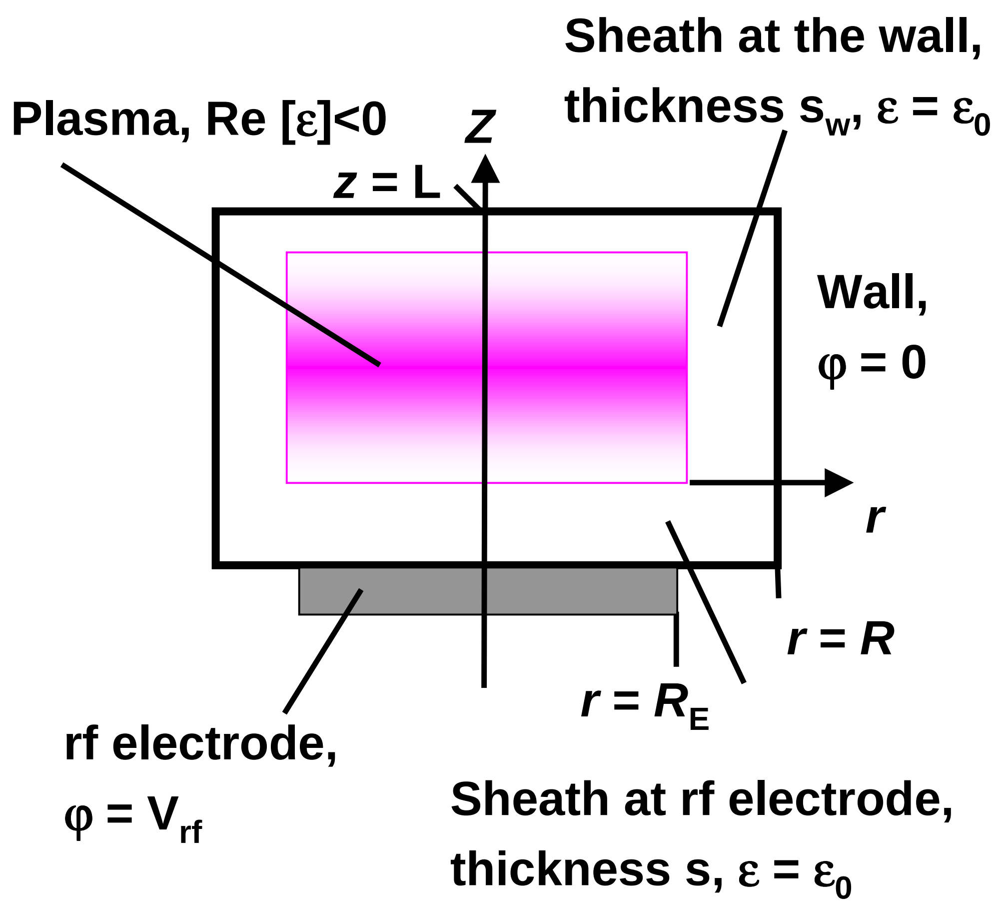

$j = -\,i\,\omega\,\nabla H$

(H ... generating function of rf density j)

Harmonic function H:

$$\nabla H = \nabla \bullet \nabla H = -\frac{\nabla \bullet j}{i\,\omega} = 0$$

$\nabla \times j = 0$, $\nabla j = 0$

➡ Laplace equation (in cylindrical coordinates)

Source: M. Klick et al., Jpn. J. Appl. Phys., Part I, 36(1997)7B, 4625.

Basic equations

RF current distribution of cylindrical RF discharge

Boundary conditions:

$$
H(r, z) = \begin{cases} H_0 & \forall \; r \le R_E \;\wedge\; z = 0 \\ H_0 \ln \dfrac{R}{r} \Big/ \ln \dfrac{R}{R_E} & \forall \; R_E < r \le R \;\wedge\; z = 0 \\ 0 & \forall \; r \le R \;\wedge\; z = L \\ 0 & \forall \; r \le R \;\wedge\; 0 \le z \le L \end{cases}
$$

Series solution:

$$
H(r, z) = \sum_k J_0(kr)\,(A_k \cosh kz + B_k \sinh kz)
$$

Source: M. Klick et al., Jpn. J. Appl. Phys., Part I, 36(1997)7B, 4625.

ADVANCED SEMICONDUCTOR INSTRUMENTS

Basic equations

Plasma body properties

Plasma frequencies: $$\omega_{e,i} = \left(\frac{n_{e,i}\, e^2}{m_{e,i}\, \varepsilon_0} \right)^{1/2}, \quad \omega_i \ll \omega \ll \omega_e$$

Hydrodynamic approach and cold plasma approximation for the electrons in the plasma body

Permittivity of plasma body, Re [ε]<0: $$\frac{\varepsilon_0}{\varepsilon} = 1 - \frac{\omega_e^2(\vec{r})}{\omega(\omega - i\nu_e)}$$

Continuation of displacement *D*: $\nabla D = \nabla \bullet (\varepsilon E) = \varepsilon \nabla \bullet E + E \bullet \nabla \varepsilon = 0$

Inhomogeneous plasma body $$\left| \frac{\nabla E}{E} \right| \gg \left| \frac{\nabla n_e}{n_e} \right| \approx \left| \frac{\nabla \varepsilon}{\varepsilon} \right|$$

or $\varepsilon = f(\varphi)$.

Source: M. Klick et al., Jpn. J. Appl. Phys., Part I, 36(1997)7B, 4625.

ASI
ADVANCED SEMICONDUCTOR INSTRUMENTS

Basic equations

Plasma body impedance

Average density, analog to one-dimensional case:

$$\tilde{n} = \frac{n_0 - n_0}{\ln (n_0 / n_R)}$$

Neglecting displacement current in plasma body:

$$(\omega_e / \omega)^2 >> 1 + (\nu / \omega)^2$$

Neglecting higher eigenvalues of the series solution and calculation of the whole current results in the impedance of the plasma body (R_E: electrode radius):

$$\boxed{Z = \frac{m_e\, l}{\tilde{n}\, e^2\, \pi\, R_E^2}\,(i\omega + \nu)}$$

Effective length of plasma body, R radius of chamber, x_0 = 2.405, first zero of J_0:

$$l \approx \frac{R}{x_0} \tanh \frac{x_0\, L}{n_e}$$

Resisitive part ⇒ electron collision rate ν,
Inductive part ⇒ angular frequency iω.

Source: M. Klick et al., Jpn. J. Appl. Phys., Part I, 36(1997)7B, 4625.

ADVANCED SEMICONDUCTOR INSTRUMENTS

Novel Feature of Hercules 2.4

SEERS model adaptation to different etch tools

different RF current distributions

effective length of plasma body

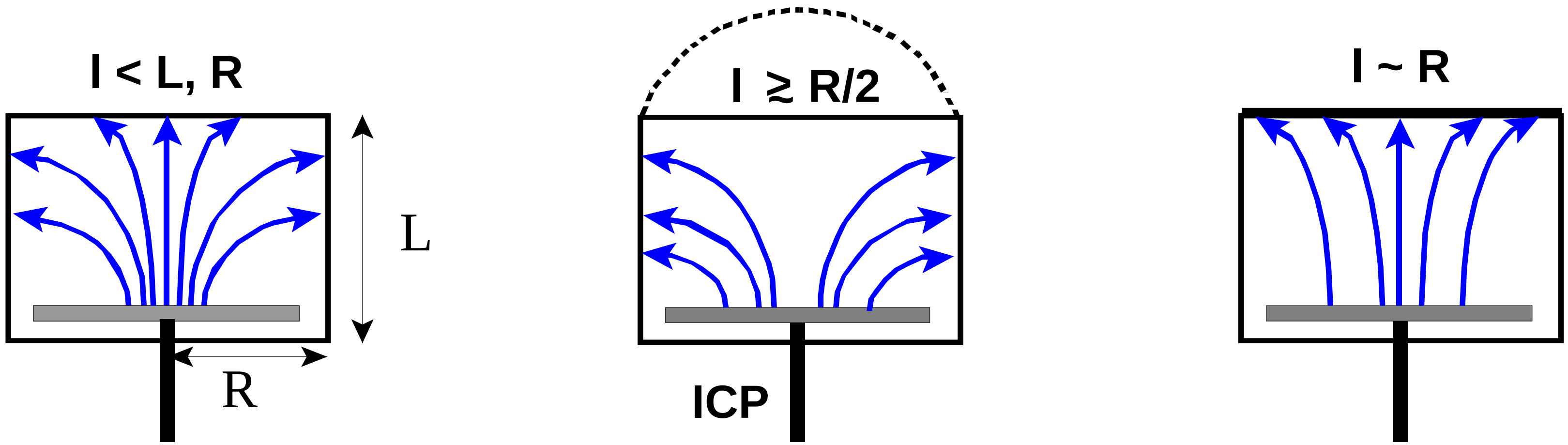

RIE	inductive coupling on top - LAM TCP - Applied Materials DPS	STS ICP
icpmode = 0	icpmode = 1	icpmode = 2

Source: M. Klick, WORKSHOP on SEERS, Infineon Technologies, Dresden, 1999

Basic equations

The characteristic equations of SEERS

Normalized inductive (Λ) and resitive (ρ) part of impedance

$$\Lambda = \frac{n_0}{\tilde{n}} \frac{l}{\lambda_D} \frac{\omega}{\omega_e}, \quad \rho = \frac{n_0}{\tilde{n}} \frac{l}{\lambda_D} \frac{\nu_e}{\omega_e}, \quad \Omega = \frac{\omega_{rf}}{\omega_e}, \quad \mu = \frac{\omega}{\omega_{rf}}$$

Displacement current of the rf sheath:
(J. Appl. Phys. 79, 3445 (1996))

$$\boxed{\Gamma_d = \frac{\Omega}{\delta(\eta_s)} \frac{d\eta_s}{d\tau}}$$

Characteristic equation in frequency domain (* denotes convolution):

$$\boxed{i\mu\eta_{rf} = \Omega^{-1}\delta * \Gamma + i\mu\rho\Gamma - \mu^2\Lambda}$$

Source: M. Klick et al., Jpn. J. Appl. Phys., Part I, 36(1997)7B, 4625.

The RF sheath

Introduction

Debye length:

$$\lambda_D = \left(\frac{\varepsilon_0 \, k \, T_e}{n_0 \, e} \right)^{1/2} \quad << \; L, R$$

Normalized quantities (n_0 density owing to Bohm criterion):

$$\eta = \frac{V_0 - V}{k \, T_e / e} \quad , \; \delta = \frac{s}{\lambda_D} \, , \quad \tau = \omega_{rf} \, t.$$

$$\Gamma = \frac{j}{j_{es} \, (2\pi)^{1/2}} \; , \; (2\pi)^{1/2} \, j_{es} = e \, n_0 \, \lambda_D \, \omega_e = e \, n_0 \left(\frac{k \, T_e}{m_e} \right)^{1/2} .$$

Source: M. Klick et al., Jpn. J. Appl. Phys., Part I, 36(1997)7B, 4625.

Advanced Semiconductor Instruments

The RF sheath

Displacement current of the RF sheath

Displacement current density j_d in the sheath in units of the Maxwellian electron saturation current density j_{es} at $\xi = 0$:

$$\Gamma_d = \frac{j_d}{(2\pi)^{1/2} j_{es}} \qquad (1)$$

The electron current density can be expressed as

$$(2\pi)^{1/2} j_{es} = e\, n_0\, \lambda_D\, \omega_e = e\, n_0 \left(\frac{k\,T_e}{m_e}\right)^{1/2} . \qquad (2)$$

Restriction of vanishing displacement current:

$$\underset{\xi<\xi_1}{\forall}\, \Gamma_d(\xi) = 0 \Leftrightarrow \underset{\xi<\xi_1}{\forall} \left(\frac{d\,\zeta}{d\,t}\right) = 0 \Longrightarrow \left(\int_0^{\xi_1} \frac{d\,\zeta}{d\,t}\, d\xi = \frac{\partial\, \eta'_1}{\partial\, t} = 0\right) \qquad (3)$$

η'_1 denotes $d\eta / d\xi$ for $\xi = \xi_t$ (ξ_t is a function of time).

Source: M. Klick et al., Jpn. J. Appl. Phys., Part I, 36(1997)7B, 4625.

The RF sheath

Displacement current and sheath thickness

$$\Gamma_d = \frac{1}{\omega_e} \frac{d}{dt} \int_0^{\xi_w} \zeta \, d\xi = \frac{1}{\omega_e} \frac{d}{dt} \left(\int_0^{\xi_1 - 0} \zeta \, d\xi + \int_{\xi_1 + 0}^{\xi_w} \zeta_+ \, d\xi \right) \qquad (4)$$

Known relation for Γ_d depending on sheath width and ion density:

$$\boxed{\begin{gathered} \Gamma_d = - \frac{\zeta_{+1} - \zeta_1}{\omega_e} \frac{d\xi_1}{dt} \\ \zeta_{+1} \doteq \zeta_+ (\xi_1 + 0) \qquad \zeta_1 \doteq \zeta_+ (\xi_1 - 0) \end{gathered}} \qquad (5)$$

Source: M. Klick et al., Jpn. J. Appl. Phys., Part I, 36(1997)7B, 4625.

ADVANCED SEMICONDUCTOR INSTRUMENTS

Sheath potential

RF potential and sheath thickness

Avoiding to calculate explicitly ion and sheath width, integrating the POISSON equation yields for $\xi > \xi_1$:

$$\eta(\xi, t) = \int_0^{\xi} \int_0^{\mu} \zeta(\nu)\, d\nu\, d\mu = \int_{\xi_1+0}^{\xi} \int_{\xi_1+0}^{\mu} \zeta_+(\nu)\, d\nu\, d\mu + \eta(\xi_1, t) + \eta'_1(\xi_1)\,(\xi - \xi_1) \qquad (6)$$

and at $\xi > \xi_w$:

$$\eta(\xi_w, t) = \eta_w(t) = \int_{\xi_1+0}^{\xi_w} \int_{\xi_1+0}^{\mu} \zeta_+(\nu)\, d\nu\, d\mu + \eta(\xi_1, t) + \eta'(\xi_1)\,(\xi - \xi_1) \qquad (7)$$

Source: M. Klick et al., Jpn. J. Appl. Phys., Part I, 36(1997)7B, 4625.

The RF sheath

Displacement current and RF potential

Differentiation with respect to ξ_1 for $\xi > \xi_1$:

$$\frac{d\eta}{d\xi_1} = -\zeta_{+1}(\xi - \xi_1) + \frac{d\,\eta'_1}{d\xi_1}(\xi - \xi_1) = -(\zeta_{+1} - \zeta_1)(\xi - \xi_1) \qquad (8)$$

and at $\xi > \xi_w$:

$$\frac{d\eta_w}{d\xi_1} = -\zeta_{+1}(\xi_w - \xi_1) + \frac{d\,\eta'_1}{d\xi_1}(\xi_w - \xi_1) = -(\zeta_{+1} - \zeta_1)(\xi_w - \xi_1) \qquad (9)$$

Introduction sheath width $\delta = \xi_w - \xi_1$ depending on the sheath voltage η_w in conjunction with Eq. (5):

$$\boxed{\Gamma_d = -\frac{1}{\omega_e(\xi_w - \xi_1)}\frac{d\eta_w}{d\,t} = \frac{1}{\omega_e\,\delta}\frac{d\eta_w}{d\,t} \qquad (10)}$$

This relation is independent of the density distribution $\zeta_{e,+}$ and is not a simple extension of that for a capacitance with movable plates (no function of $d\delta/\,d\eta_w$).

Source: M. Klick et al., Jpn. J. Appl. Phys., Part I, 36(1997)7B, 4625.

Advanced Semiconductor Instruments

The RF sheath

Generalized model I

Known models based on the approximation density by a step-wise profile. For steady state ion distribution, where $\omega >> \omega_i$, this disadvantage can be avoid.

POISSON equation can be transformed into the equivalent integral equation:

$$\eta_w = \int_{\xi_0}^{\xi_w} (\xi_w - \nu)\, \zeta(\nu)\, d\nu + \eta(\xi_0) + \frac{d\,\eta(\xi)}{d\xi} , \qquad (11)$$

Potential and field strength at ξ_0 are boundary conditions (ξ_0 outside sheath) introducing the displacement flux at the wall as the net charge in the sheath:

$$\Psi_w = \int_{\xi_0}^{\xi_w} \zeta(\xi)\, d\xi , \qquad (12)$$

Relation between displacement current and displacement flux:

$$\Gamma_d = - \frac{1}{\omega_e} \frac{d\Psi_w}{d\,t} . \qquad (13)$$

Source: M. Klick et al., Jpn. J. Appl. Phys., Part I, 36(1997)7B, 4625.

Advanced Semiconductor Instruments

The RF sheath

Generalized model II

Exact definition of the dynamic sheath boundary δ:

$$\delta = \frac{d\eta_w}{d\Psi_w} \quad , \qquad (14)$$

Distance to wall: $x = \xi_w - \xi,\ \zeta_x(x) = \zeta(\xi_w - x)$.

$$\delta = \frac{\int_0^{\hat{\delta}} \frac{\partial \zeta_x(x,t)}{\partial t}\, x\, dx}{\int_0^{\hat{\delta}} \frac{\partial \zeta_x(x,t)}{\partial t}\, dx} \qquad (15)$$

- **assumption of a wise distribution of electrons within the sheath,**
- **precondition: explicit dependence of the electron density on the potential, e.g., Boltzmann distribution.**

Source: M. Klick et al., Jpn. J. Appl. Phys., Part I, 36(1997)7B, 4625.

Parameter delivered by Hercules

reciprocally spatially averaged

Electron density:

$$\tilde{n} \approx \left(\frac{1}{V} \int_V n^{-1} \, dV \right)^{-1}$$

Electron collision rate:

$$\tilde{\nu} \approx \frac{\tilde{n}}{V} \int_V \frac{\nu}{V} \, dV$$

Bulk power:

$$P_B \propto \frac{\tilde{\nu}}{\tilde{n}} \sum \left[I^{(k)} \right]^2$$

ADVANCED SEMICONDUCTOR INSTRUMENTS

Meaning of fundamental plasma parameters

Reciprocal averaged values

Electron density n_e:

$$\tilde{n} \approx \left(\frac{1}{V}\int_V n^{-1}\, dV \right)^{-1}$$

- proportional to ion currents
- simple correlation with etch rate in the case of dominating „physical“ (sputter) etching

Collision rate:

$$\tilde{\nu} \approx \frac{\tilde{n}}{V}\int_V \frac{\nu}{n}\, dV$$

- interaction between electrons and neutrals
- impact of electrons on chemistry
- feedback from chemistry via cross sections and relative concentration of species

stochastic heating (sheath)

electron temperature

gas pressure

$$\nu = \nu_{stoch} + \sqrt{\frac{8\,kT_e}{\pi\, m_e}}\,\frac{p}{kT_N}\sum_k \frac{p_k}{p}\sigma_k$$

gas temperature

relative concentration

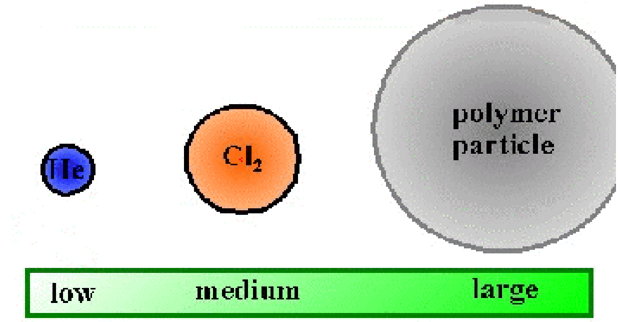

Depending of collision rate on tool parameters

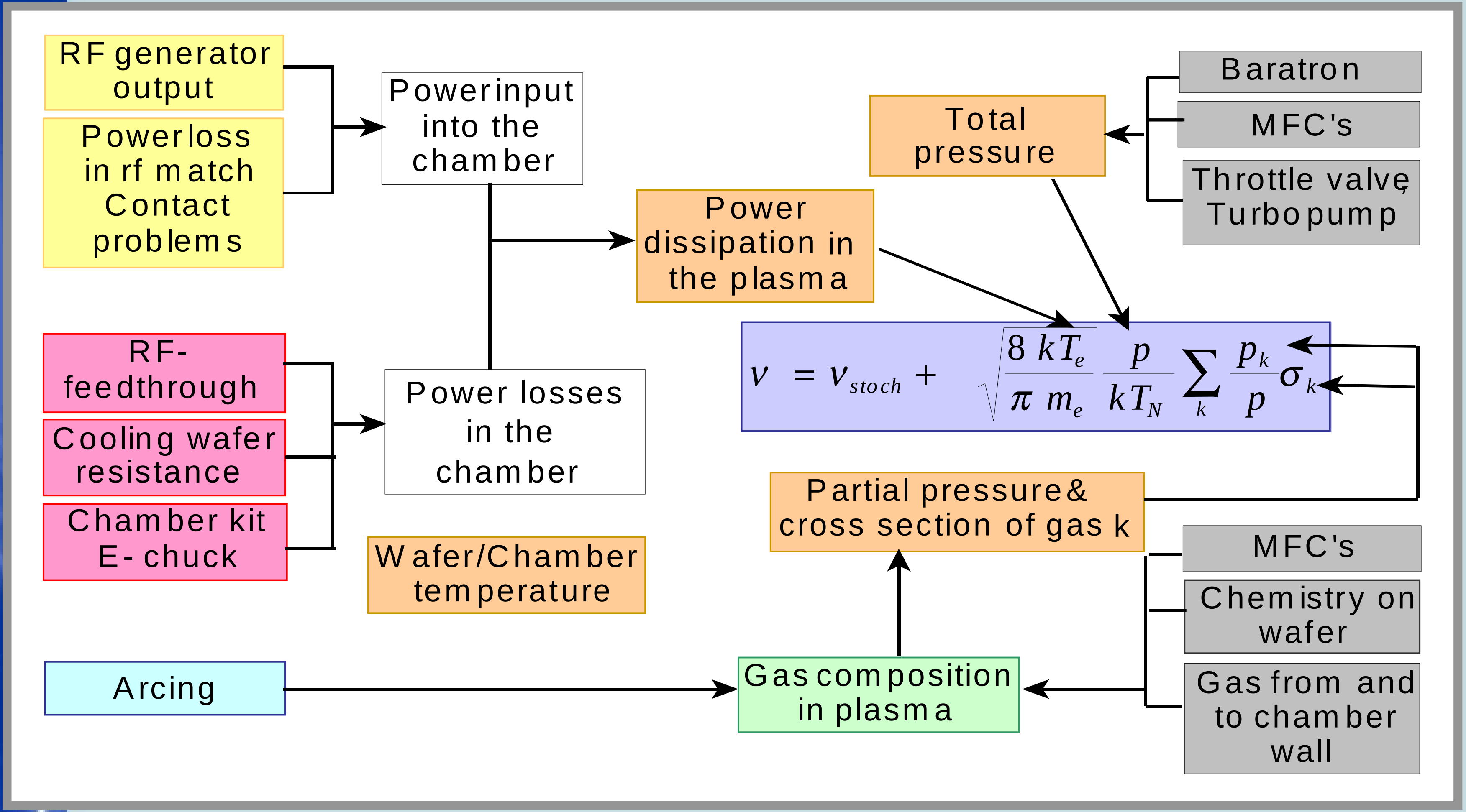

Hardware and Installation

Sensor at
Lam TCP 9600SE

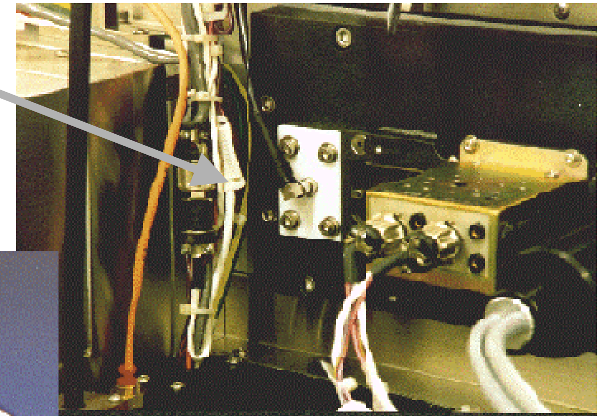

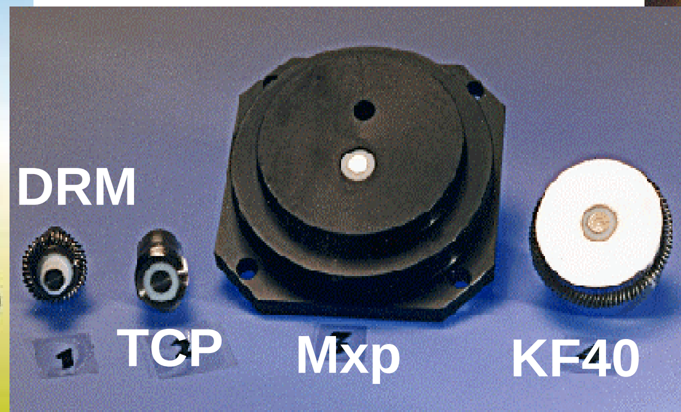

Sensor
- easy setup and installation for different tools
- insensitive to deposition insulating layers (polymers)
- passive and removable internal plasma parameters

HERCULES Sensor Types form LAM TCP

RF current sensor
for LAM TCP

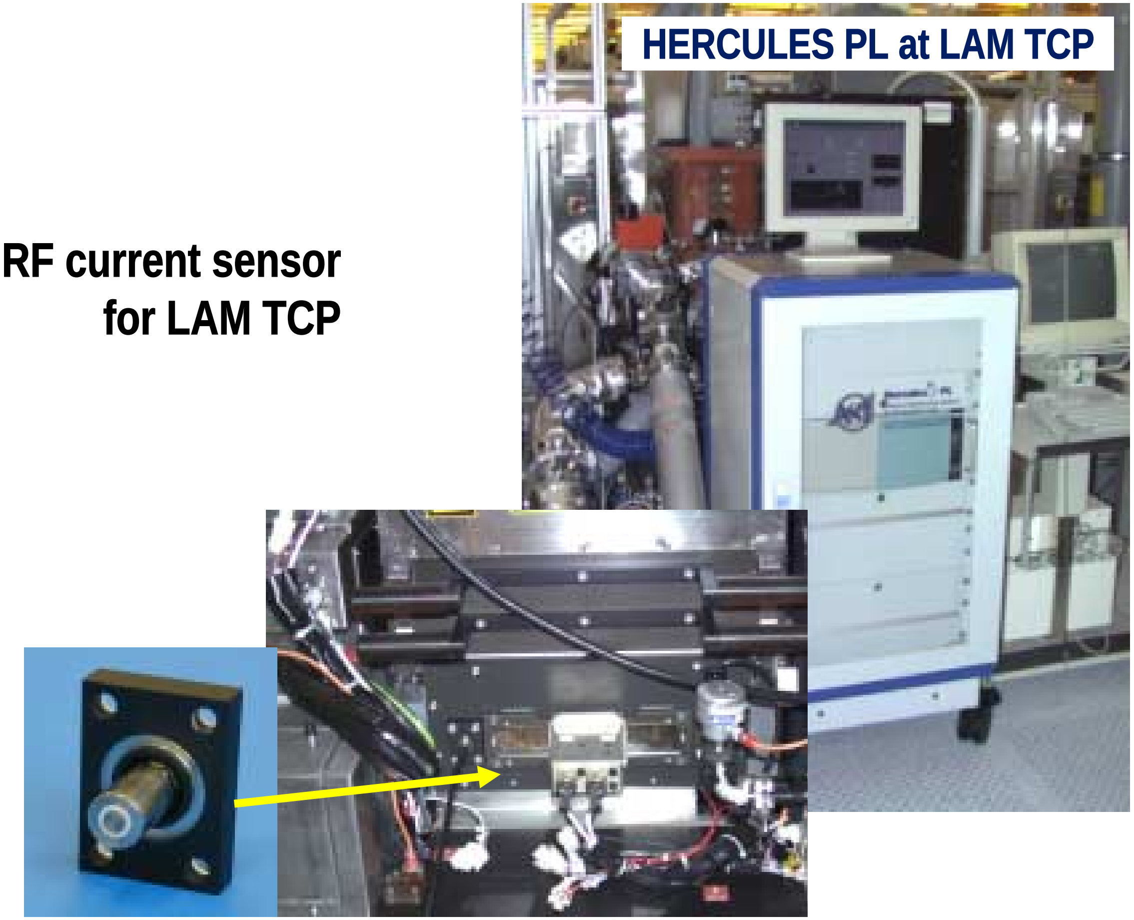

Source: U. Nehring, AEC/APC-Symposium XII, 2000, USA

Adaption of HERCULES Sensor Types

Surfaces: anodized aluminum, similar to chamber wall

DPS
- peak voltage
- inductively coupled
- capacitive ≠ inductive coupled frequency

LAM 300
- peak voltage
- inductively coupled
- special software interface

eMxP+
- peak voltage
- rotating B-field
- optical access for OES

Source: V. Tegeder, AEC/APC-Symposium XII, 2000, USA

ADVANCED SEMICONDUCTOR INSTRUMENTS

ADVANCED SEMICONDUCTOR INSTRUMENTS

Insulating layer on sensor

13 MHz

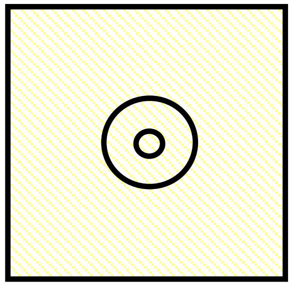

1 kHz

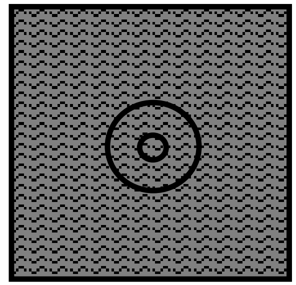

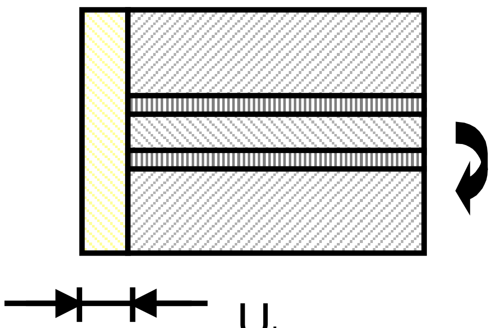

$Z_{ins} << 50$ Ohm

$\frac{U_{ins}}{U_{sens}} << 1$ → no influence

$d << s$ → no influence

d: polymer sheath thickness

s: space charge sheath thickness ~ 1mm

Comparison of Langmuir probe and SEERS

Experimental setup

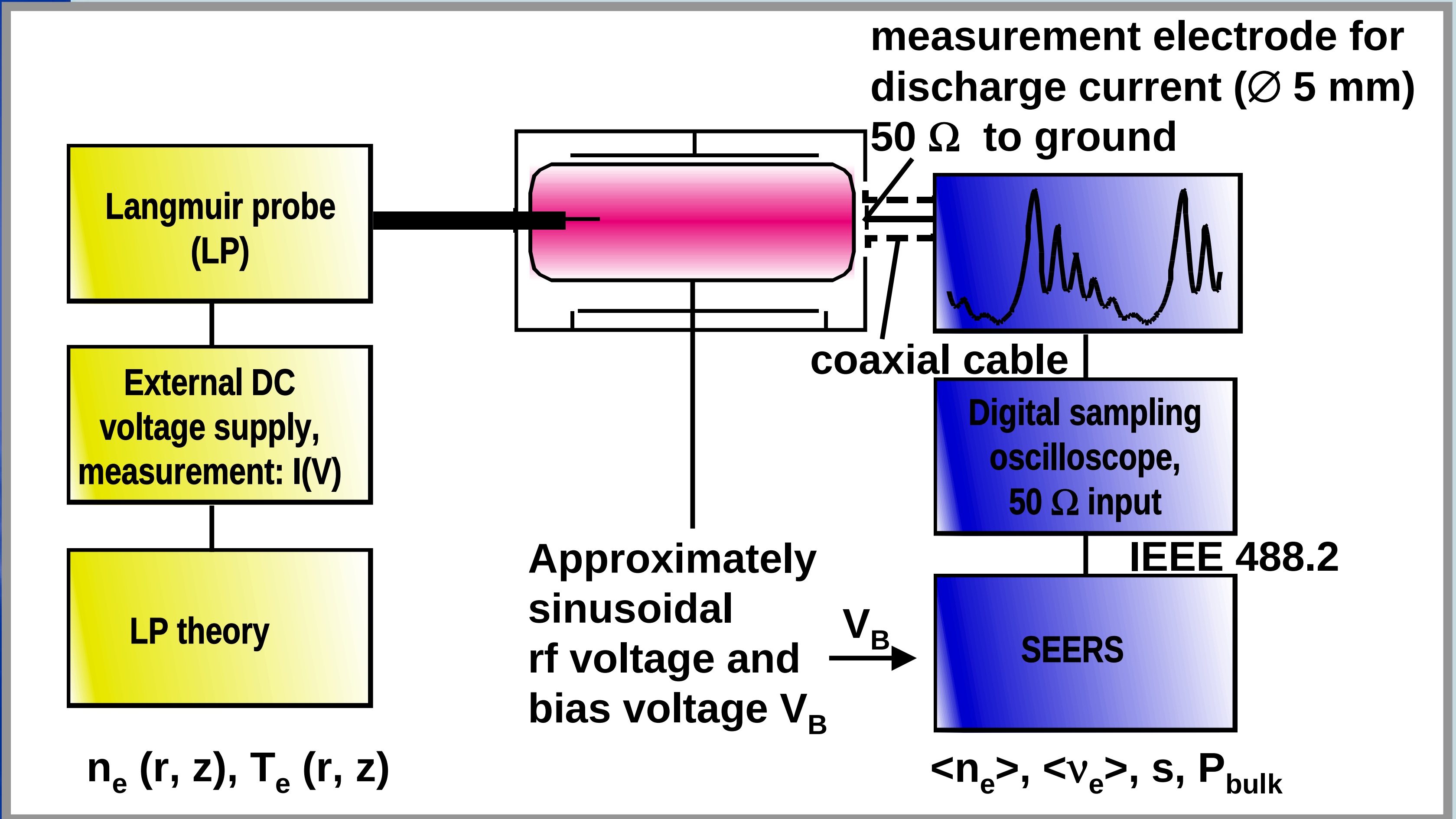

Source: M. Klick et al., Jpn. J. Appl. Phys., Part I, 36(1997)7B, 4625.

Comparison of Langmuir probe and SEERS

Electron density and collision rate vs. bias voltage

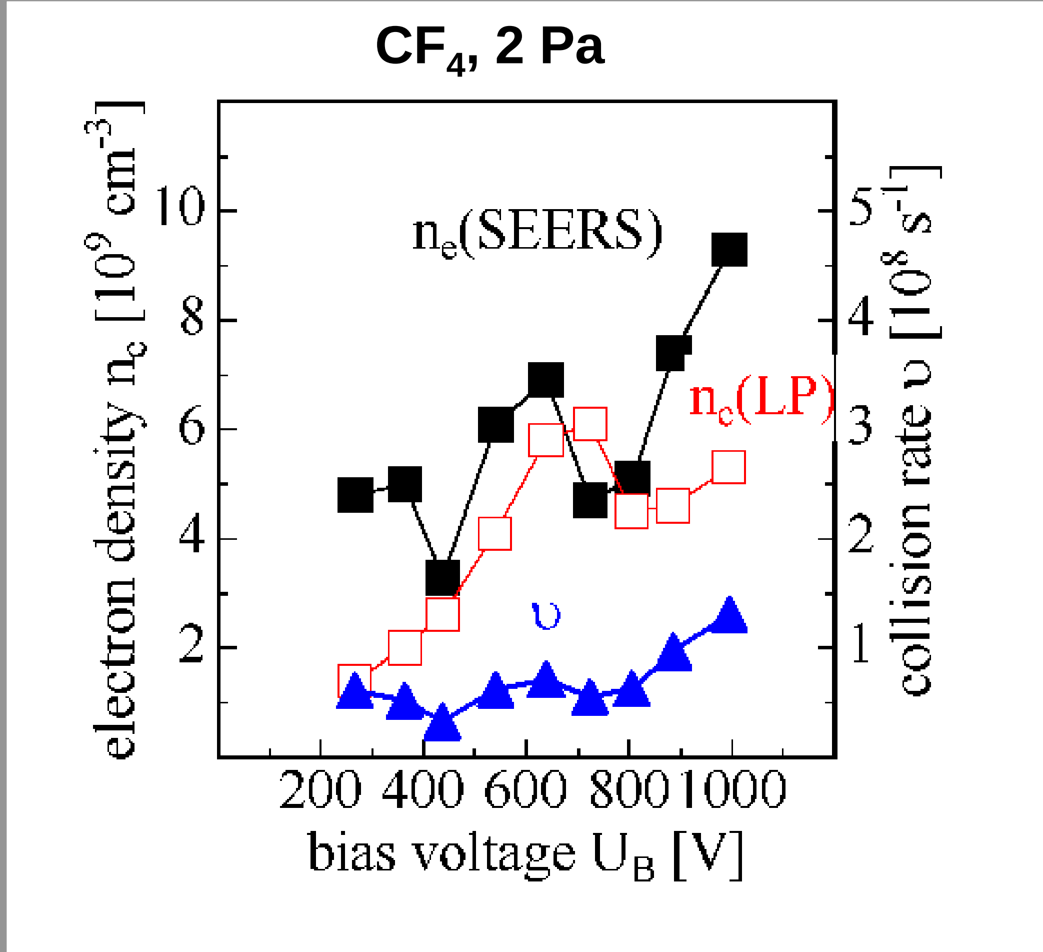

RIE, 13.56 MHz, electrode diameter 15.5 cm, chamber diameter 30 cm, electrode gap 6.7 cm.

For CF_4, which is much more complex because of the high fragmentation, the discharge is slightly less stable yielding anincreased error of both methods.
A second known reason is the rising density of negative ions resulting in a different axial density profile in the bulk plasma of CF_4.

Source: M. Klick et al., Jpn. J. Appl. Phys., Part I, 36(1997)7B, 4625.

Arcing detection

No arcing

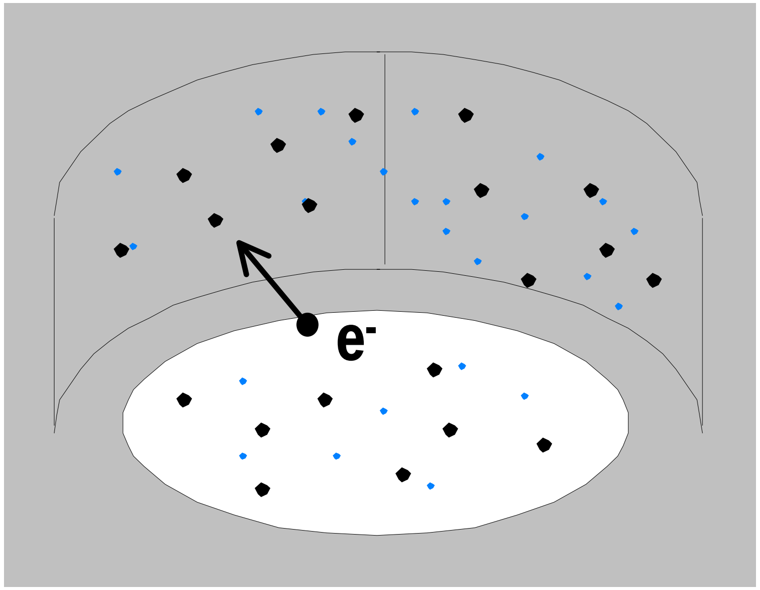

Process gas

In case of arcing - Impact on collision rate

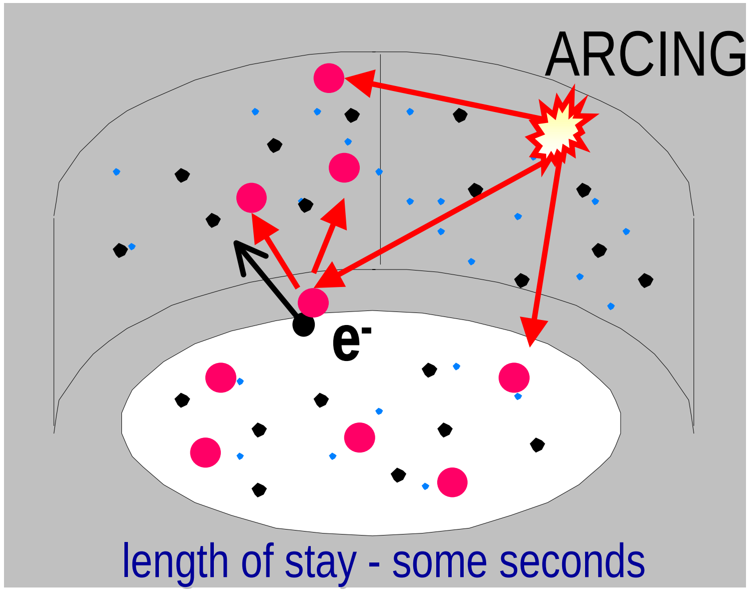

Process gas and polymer

Fast Tool start up

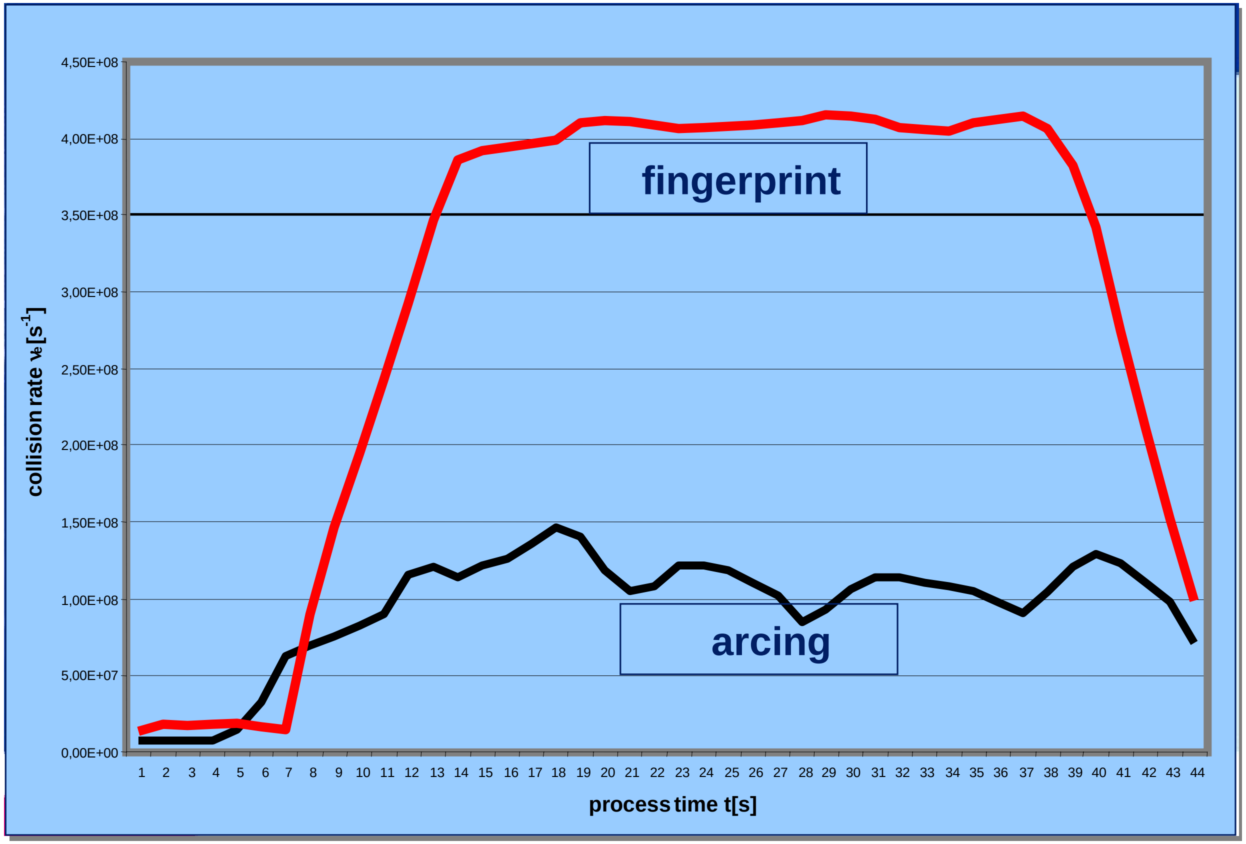

Arcing detected at new tool

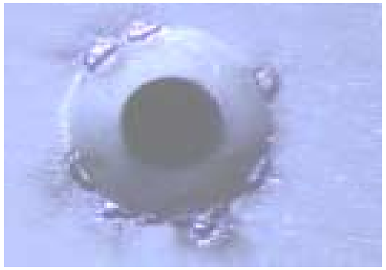

Arcing traces at gas distribution

Recipe

Step 1

25mtorr / 215W / 30G/ 50 sccm O2

Step 2

25mtorr / 215W / 0G/ 50 sccm O2

Source: V. Tegeder, AEC/APC-Symposium XII, 2000, USA

by courtesy of AMD

LAM TCP 9600SE, metal etch

Electron density and bulk power vs. TCP power

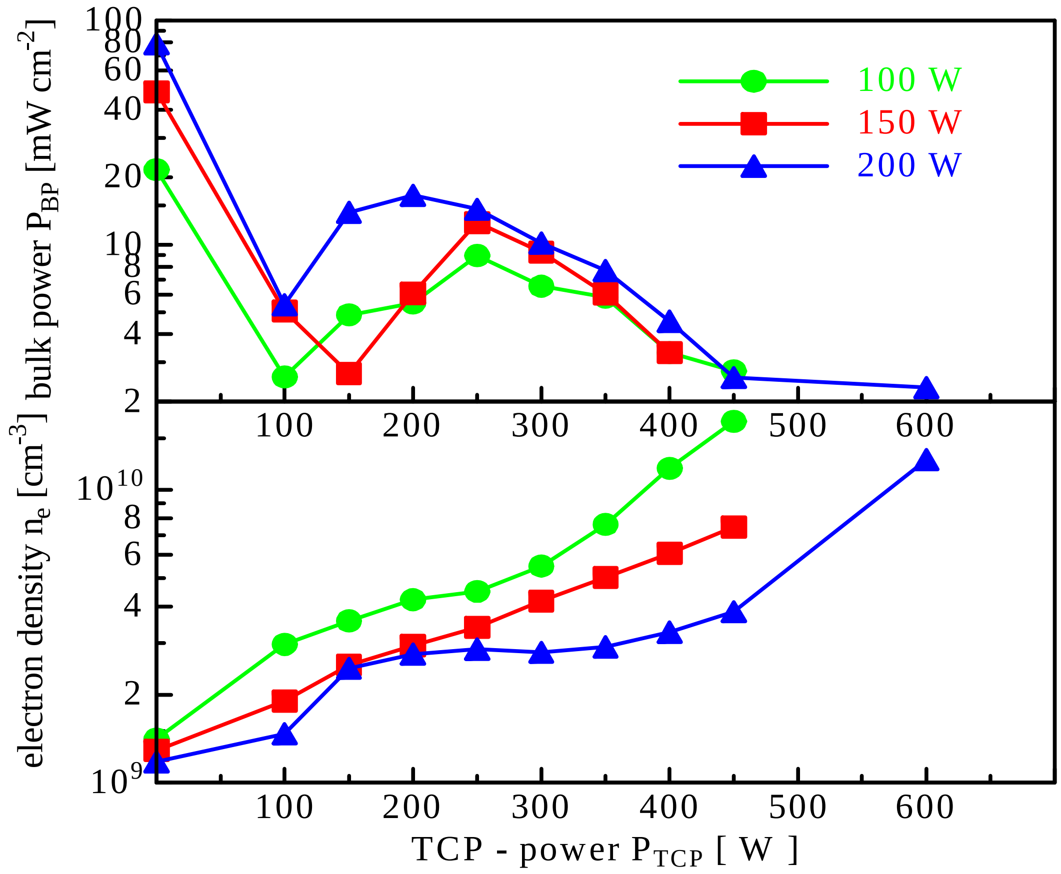

TCP power effects the density and collision rate of electrons and therefore the plasma impedance and the power dissipation of the bottom power (capacitive).

Mainly dependent on collision rate, the bulk power (bottom) decreases for increasing TCP power (>250W). This is the reason for the plateau in the electron density.

Source: S. Wurm, Lam Research Corp., 10th Ann. European Techn. Symp., Geneva, Switzerland, 1998.

ASI
Advanced Semiconductor Instruments

Plasma parameters before and after chamber cleaning

Impact of background chemistry

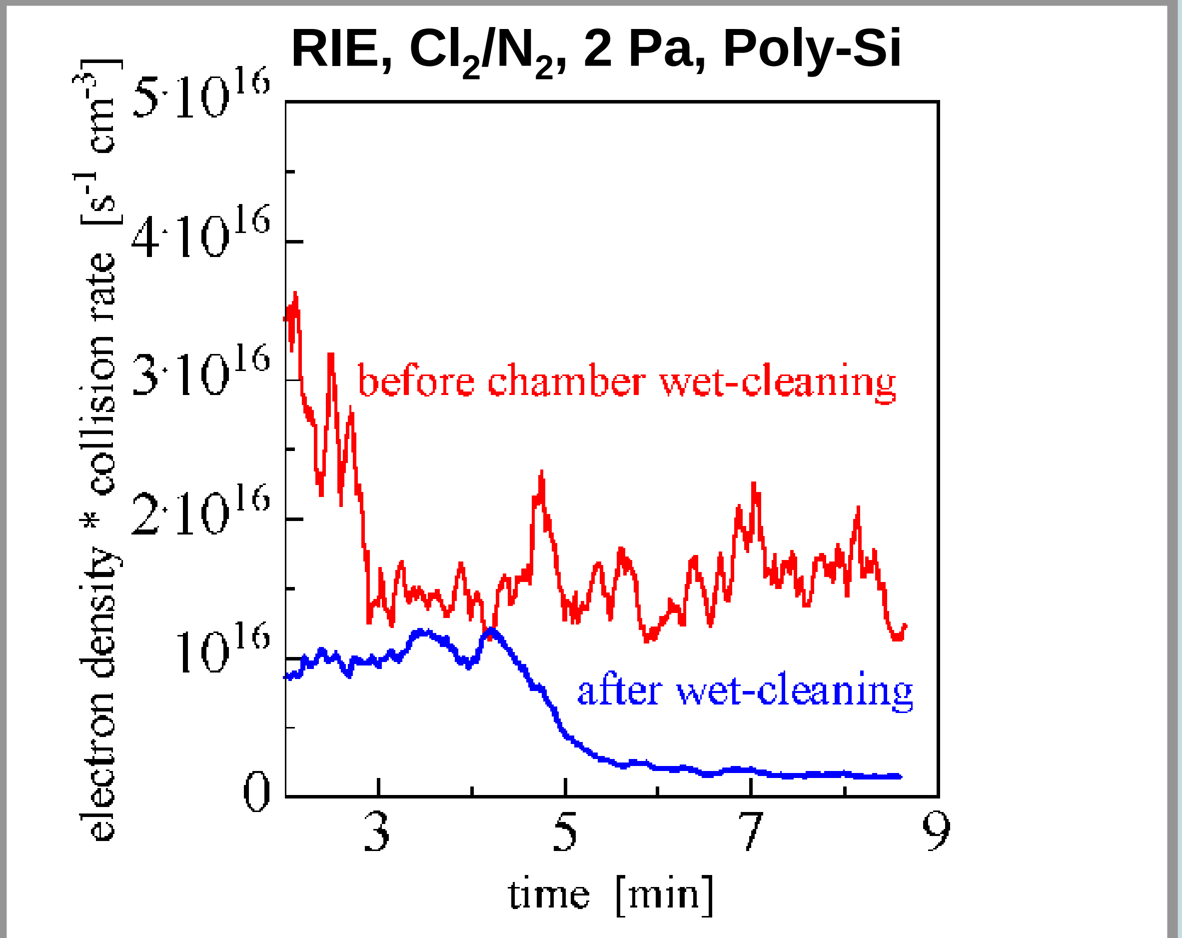

The internal plasma parameters monitored during two standard dry-cleaning steps are shown.
Before wet-cleaning of the chamber there is no pure HI plasma, it is strongly influenced
by removing of deposited layers on the chamber wall.
After wet-cleaning the plasma is stable and removes the remaining contamination and solvents within five minutes.

Source: I. Orgzall et al., Future Fab International Vol. 2, 235, 1996

Plasma parameters during two different cleaning

Impact of background chemistry

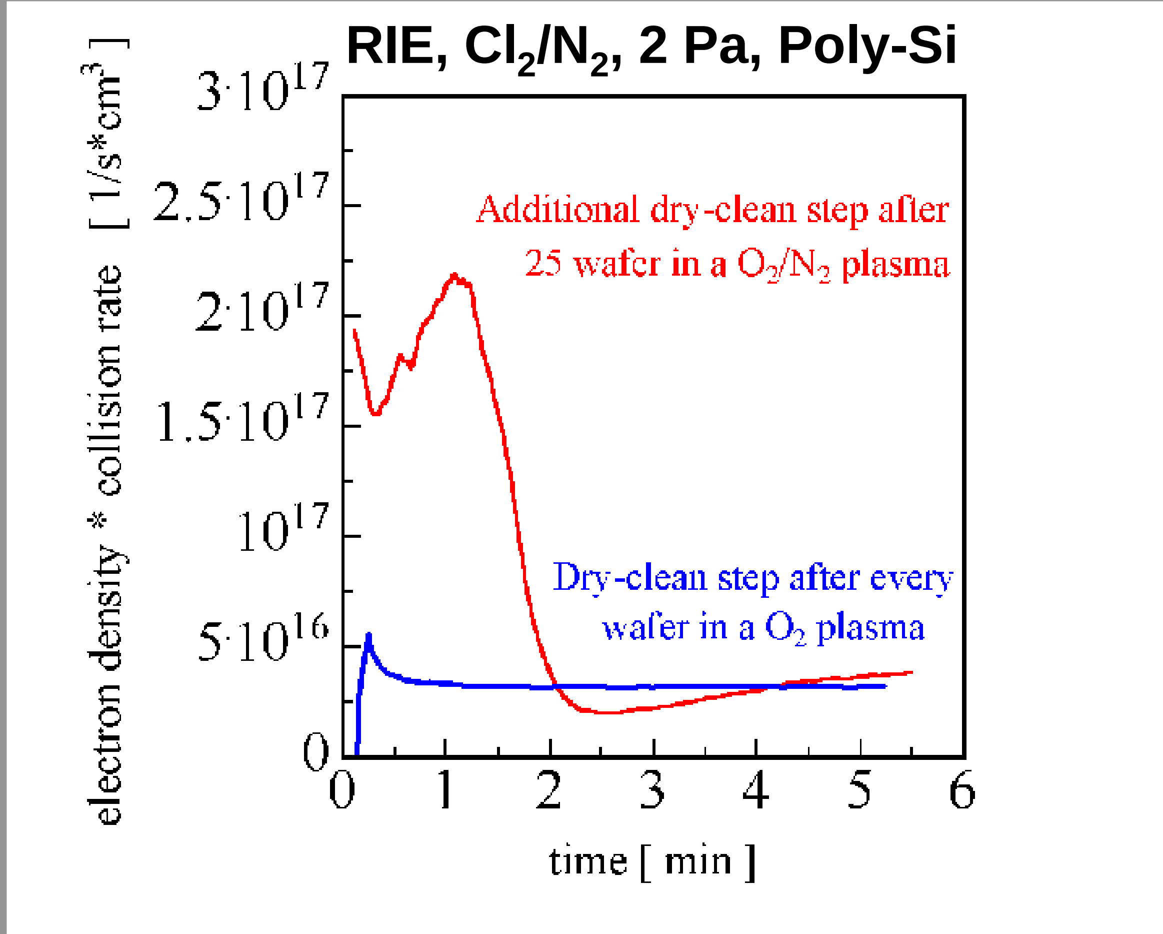

The internal plasma parameters monitored during two standard dry-cleaning steps are shown.

The first step was realised after every etching process, the second only after 25 runs, additionally.

One can detect the efficiency of such clean steps.

Source: I. Orgzall et al., Future Fab International Vol. 2, 235, 1996

Sputter clean control for in-line PVD

For some PVD applications, plasma based cleaning process are the precondition for a stable PVD process. Using the example of razor blade production, the sputter cleaning process is shown to be a critical one. Ten thousands are treated simultaneously at carriers. This process is designed to remove residues from pre-processes, e.g., solvents. Removing the residues as well as sputter effects at the blade and carrier surfaces leads to the deposition of a metal-organic layers at the chamber wall. The process chamber investigated is part of a high throughput in-line sputter tool. Owing to the resulting aging of the process chamber, cleaning procedures are often necessary.

secondary plasmas

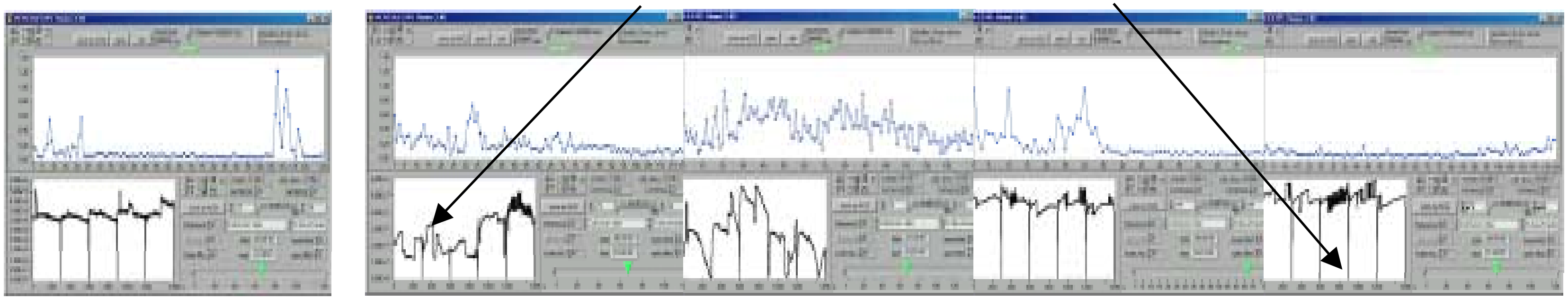

Long term monitoring of averaged collision rate (one point one carrier)

Source: P. Krenzlin, Gillette, AEC/APC Workshop Europe, Dresden, 2000.

Sputter clean control for in-line PVD

This work presents long term trends of plasma parameters provided by the plasma monitoring system Hercules/PL using a passive sensor mounted in a KF 40 standard flange. The Hercules system is insensitive to deposited layers and is mounted flat in the wall. The automatic monitoring system includes an on-line and model based data compression. The most sensitive parameter, determined in real-time, is the electron collision rate, whereas the electron density was on a comparable constant level of 10^9 cm^{-3}.

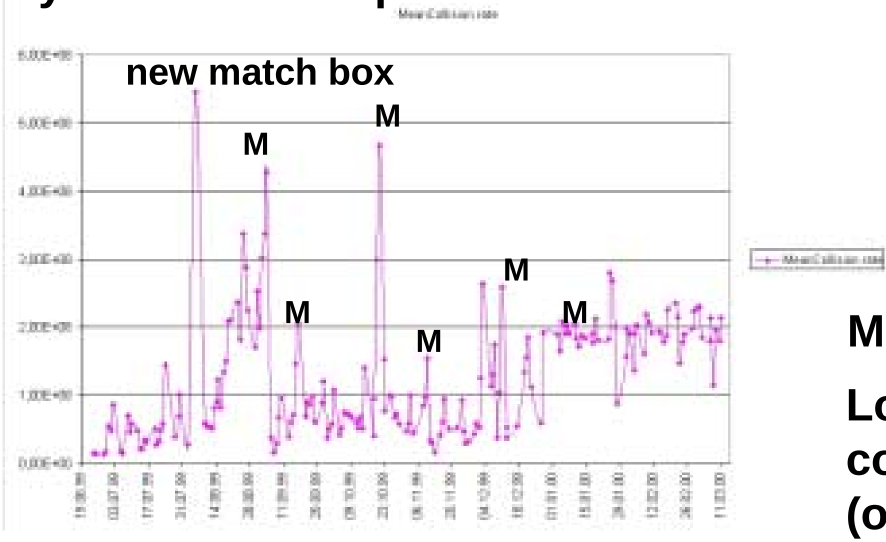

M: Maintenance

Long term monitoring of collision rate
(one point one day)

Sputter clean control for in-line PVD

The impact of chamber cleans and the following reconditioning of the chamber are the main focus. Regular cleans including the replacement of chamber parts and quick clean are shown to lead to different results. The duration of the real conditioning of the chamber by empty carriers and the slowly growing stability of the process after a cleaning procedure are shown clearly. The occurrence of parasitic plasmas was found to be one significant indicator of process stability.

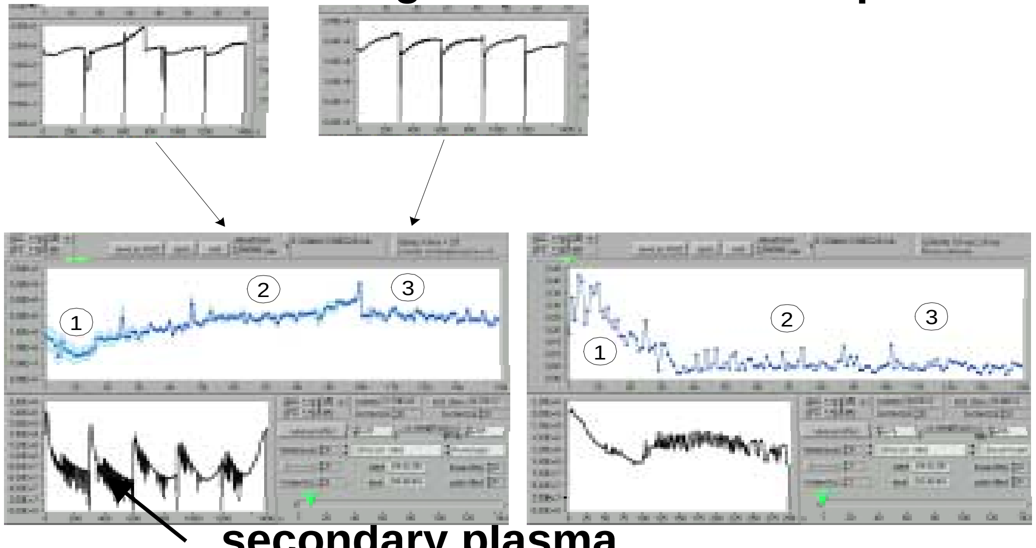

1. Conditioning of carriers after tool cleaning (phase 1)
2. Tool conditioning (phase 2)
3. Start of production with complete carriers (phase 3)

Source: P. Krenzlin, Gillette, AEC/APC Workshop Europe, Dresden, 2000.

Applications

- Development and optimizing processes	yes
- Long and short term tool stability	yes
- Tool & chamber matching	yes
- Control of chamber cleaning	yes
- Control of power coupling into plasma	yes
- Endpoint detection	possible
- Layer resolution	possible
- Uniformity	yes
- Reduction of test- and monitor wafers	yes
- Detection of tool failure	yes
- Arcing detection	yes
- Fault classification detection	yes

Benefit using Hercules

Summary

- SEERS uses a general hydrodynamical (fluid) discharge model.
- The measured parameters are ***absolute*** values.
- The measured parameters depend significantly on chamber conditions and etch results.
- No difficult modeling by the user is necessary, results are available immediately.

Thank to Stefan Wurm, International Sematech, Andreas Steinbach, Infineon Technologies Dresden, Bernard Auda, IBM Essonnes, Mathias Hofman AMD, and Mike Robbins, *Motorola*, Gerard Petit and Michel Derie, *STM* for providing production data and diagrams and for helpful discussions. Special thank to Dr. Marita Kammeyer for preparation and helpful discussions.